International Journal of Thermophysics, Vol. 14, No. 1, 1993

Transient Temperature Response in Functionally Gradient Materials

T. Ishiguro,[1] A. Makino,[1] N. Araki,[1] and N. Noda[2]

Received August 12, 1992

The temperature response in functionally gradient materials (FGM), subjected to pulse- or stepwise heating at the front surface, is evaluated. Applicability of the approximate solution for the temperature response is investigated by comparing it with an exact analytical solution for the FGM in which thermophysical properties have certain profiles. When the FGM is composed of conventional solid materials, appropriateness of the approximate solution for the FGM is demonstrated as far as the temperature response near the rear surface is concerned. The approximate solution is also compared with the solution for the multilayered material. It is shown that an eight-layered material can be regarded as an FGM, as far as the temperature response at the rear surface is concerned, and that the approximate solution can predict the temperature response within 6% error. Because of its simplicity and fair degree of agreement, the approximate solution is anticipated to be used not only for qualitative but also for quantitative prediction of the temperature response near the rear surface of the FGM in engineering applications.

KEY WORDS: functionally gradient material (FGM); multilayered material; pulsewise heating method; stepwise heating method; thermal diffusivity.

1. INTRODUCTION

Functionally gradient materials (FGM), which are composed of different material components such as ceramics and metals with continuous profiles in composition, structure, texture, mechanical strength, and thermophysical properties, have attracted special interest as advanced heat-shielding/structural materials in future space applications, as well as electronic materials,

[1] Department of Energy and Mechanical Engineering, Faculty of Engineering, Shizuoka University, Hamamatsu 432, Japan.
[2] Department of Mechanical Engineering, Faculty of Engineering, Shizuoka University, Hamamatsu 432, Japan.

0195-928X/93/0100-0101$07.00/0

and materials resistant to wear, corrosion, and heat. In order for an FGM to qualify as an advanced heat-shielding/structural material, its thermophysical properties as well as its mechanical properties should be evaluated properly. Transient methods, such as those involving pulse- or stepwise heating, can be used for these evaluations because of their simplicity and advantages at high temperatures. However, application of the transient methods requires great care because the thermal diffusivity obtained from the temperature response is apparent and different from that of the averaged property related to thermal resistance. Therefore, before making measurements by transient methods, it is essential to investigate and confirm the measurement principles in the application of the transient methods to FGM.

For this purpose, a series of investigations was conducted by some of the present authors. First, dominant parameters in the transient methods were identified by investigating the temperature response in the two-layered material [1]. Second, prior to the investigation of the FGM, a general analytical solution for the temperature response in the multilayered material which is subjected to the transient heating was derived [2]. This identification provided useful insight into the dependence of the temperature response on the thermophysical properties of each layer and facilitated not only confirmation of measurement principles but also future analytical studies to evaluate various effects in the measurements. Although the solution for the temperature response in the FGM has already been obtained [2], considering infinitesimal thickness for each layer, the validity of this solution must be further studied, especially from the engineering point of view.

The objectives and contributions of the present study are the following. First, recognizing that the solution derived for the temperature response in FGM is approximate, its applicability is investigated by comparing it with the exact analytical solution for FGM in which thermophysical properties have certain profiles. When the FGM is composed of conventional solid materials, appropriateness and usefulness of the solution for the FGM are shown as far as the temperature response near the rear surface is concerned. Second, by obtaining the temperature response at the rear surface of the sample materials, in which the thermophysical properties of the front and rear surfaces are given, the effect of the number of layers is investigated. It is shown that an eight-layered material can be considered to be an FGM, as far as the temperature response is concerned. Furthermore, the approximate solution can be used for the evalution of the heat-shielding properties if one can accept a maximum of about 6% error.

2. TEMPERATURE RESPONSE IN MULTILAYERED MATERIAL

Since the formulation for the multilayered material shown in Fig. 1 has already been done by Araki et al. [2], only the final solution for the temperature response is presented here. Solving a heat diffusion equation with appropriate initial and boundary conditions under conventional assumptions, we have the temperature response for the pulsewise heating as[3]

$$\theta_i(z, t) = \left(\frac{2^{i-1}Q}{\Lambda_i \eta_n}\right)\left(\frac{\sum_{j=i}^{i-1+2^{n-i}} \chi_j^*}{\sum_{j=1}^{2^{n-1}} \omega_j \chi_j}\right) V_P \tag{1}$$

where

$$V_P = 1 + 2\sum_{k=1}^{\infty}\left[\frac{\sum_{j=i}^{i-1+2^{n-i}} \chi_j^* \cos(\gamma_k \omega_j^*)}{\sum_{j=i}^{i-1+2^{n-i}} \chi_j^*}\right]\left[\frac{\left(\sum_{j=1}^{2^{n-1}} \omega_j \chi_j\right) e^{-(\gamma_k \omega_1)^2 \mathrm{Fo}}}{\sum_{j=1}^{2^{n-1}} \omega_j \chi_j \cos(\gamma_k \omega_j)}\right] \tag{2}$$

[3] Definitions of symbols are given under Nomenclature, at the end of the paper.

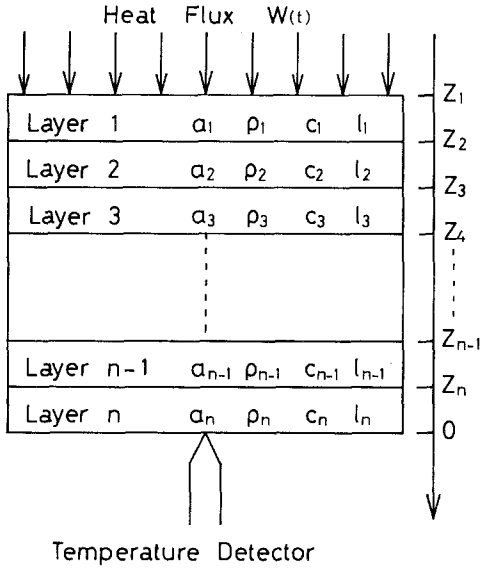

Fig. 1. Schematic diagram of the multilayered material.

is the temperature rise normalized by the maximum temperature rise at the rear surface. For the stepwise heating, we have

$$\theta_i(z,t)=\left(\frac{2^{i-1}Q\eta_n^2}{\Lambda_i\eta_n}\right)\left(\frac{\sum_{j=i}^{i-1+2^{n-i}}\chi_j^*}{\sum_{j=1}^{2^{n-1}}\omega_j\chi_j}\right)\omega_1^2 V_S \tag{3}$$

$$V_S=\mathrm{Fo}-\frac{\sum_{j=1}^{2^{n-1}}\omega_j^3\chi_j}{6\omega_1^2\sum_{j=1}^{2^{n-1}}\omega_j\chi_j}+\frac{\sum_{j=i}^{i-1+2^{n-i}}\omega_j^{*2}\chi_j^*}{2\omega_1^2\sum_{j=i}^{i-1+2^{n-i}}\chi_j^*}$$
$$-2\sum_{k=1}^{\infty}\left[\frac{\sum_{j=i}^{i-1+2^{n-i}}\chi_j^*\cos(\gamma_k\omega_j^*)}{\sum_{j=i}^{i-1+2^{n-i}}\chi_j^*}\right]\left[\frac{\left(\sum_{j=1}^{2^{n-1}}\omega_j\chi_j\right)e^{-(\gamma_k\omega_1)^2\mathrm{Fo}}}{(\gamma_k\omega_1)^2\sum_{j=1}^{2^{n-1}}\omega_j\chi_j\cos(\gamma_k\omega_j)}\right] \tag{4}$$

Here

$$\chi_j=\prod_{m=1}^{n-1}(\Lambda_{m/m+1}+\alpha_{j,m}\alpha_{j,m+1}),\qquad \omega_j=\sum_{m=1}^{n}\alpha_{j,m}\eta_{m/n} \tag{5}$$

$$\chi_j^*=\prod_{m=i}^{n-1}(\Lambda_{m/m+1}+\alpha_{j,m}^*\alpha_{j,m+1}^*),\qquad \omega_j^*=\eta_{i/n}^*+\sum_{m=i+1}^{n}\alpha_{j,m}^*\eta_{m/n} \tag{6}$$

$$\Lambda_{i/i-1}=\Lambda_i/\Lambda_{i-1},\qquad \Lambda_i=\lambda_i/\sqrt{a_i} \tag{7}$$

$$\eta_{i/n}=\eta_i/\eta_n,\qquad \eta_i=l_i/\sqrt{a_i},\qquad l_i=z_{i+1}-z_i \tag{8}$$

$$\eta_{i/n}^*=\eta_i^*/\eta_n,\qquad \eta_i^*=(z_{i+1}-z)/\sqrt{a_i} \tag{9}$$

$$\mathrm{Fo}=\frac{t}{(\omega_1\eta_n)^2} \tag{10}$$

In the above, Λ is the heat-penetration coefficient, η the thermal diffusion time, Fo the Fourier number, and γ_k the positive root of the characteristic equation

$$\sum_{j=1}^{2^{n-1}}\chi_j\sin(\gamma\omega_j)=0 \tag{11}$$

which is independent of heating methods for the front surface of the material. In Eq. (5), all combinations of $\alpha_{j,m}=\pm 1$ are to be considered for $m\geqslant 2$ while $\alpha_{j,1}=1$; in Eq. (6), all combinations of $\alpha_{j,m}^*=\pm 1$ are to be

considered for $m \geqslant i+1$ while $\alpha^*_{j,i} = 1$. Furthermore, λ is the thermal conductivity ($= \rho c a$), a the thermal diffusivity, ρ the density, c the specific heat, l the layer thickness, t the time, and z the distance from the rear surface. It should be noted that the number of j which we must take into account depends on the number n of layers; $j = 2^{n-1}$.

3. APPROXIMATE SOLUTION FOR TEMPERATURE RESPONSE IN FGM

The solution for the multilayered material can be extended for the FGM, which has continuous profiles in composition, structure, texture, mechanical strength, and thermophysical properties, if we consider the infinitesimal thickness of each layer. As derived in the Appendix, the temperature response for pulse heating is expressed as

$$V_{\mathrm{P}} = 1 + 2 \sum_{k=1}^{\infty} (-1)^k \cos(k\pi\zeta)\, e^{-(k\pi)^2 \mathrm{Fo}} (1 + \Phi_{\mathrm{P},k}) \tag{12}$$

and that for stepwise heating as

$$V_{\mathrm{S}} = \mathrm{Fo} - \frac{1 + \Phi_{\mathrm{S},0}}{6} + \frac{\zeta^2}{2} - 2 \sum_{k=1}^{\infty} \frac{(-1)^k \cos(k\pi\zeta)}{(k\pi)^2} e^{-(k\pi)^2 \mathrm{Fo}} (1 + \Phi_{\mathrm{S},k}) \tag{13}$$

where

$$\zeta = \frac{1}{\eta_L} \int_z^0 \frac{dz}{\sqrt{a(z)}}; \qquad \eta_L = \int_{-L}^0 \frac{dz}{\sqrt{a(z)}} \tag{14}$$

and

$$\mathrm{Fo} = \frac{t}{\eta_L^2} \tag{15}$$

is the Fourier number. In the above, η_L is the total thermal diffusion time, ζ is the normalized thermal diffusion time from a certain point in the FGM to its rear surface, and correction terms Φ_{P}, $\Phi_{\mathrm{S},0}$, and $\Phi_{\mathrm{S},k}$ are expressed by Eqs. (A16), (A20), and (A21), respectively.

Note that Eqs. (12) and (13), without correction terms Φ's, are first derived by Araki et al. [2] under the equi-heat-penetration assumption of $\Lambda_{m/m+1} \approx 1$, which yields $\chi_1 \gg \chi_j$ and $\gamma_k \omega_1 \approx k\pi$. It is also noted that these approximate solutions coincide with those for the single-layered material.

4. TEMPERATURE RESPONSE IN FGM WHEN AN EXACT ANALYTICAL SOLUTION EXISTS

In order to evaluate the validity of the approximate temperature response shown in Eq. (12) for the pulse heating [or in Eq. (13) for the step heating], a comparison between the approximate and the exact analytical solutions must be made. To do so, we are required to find an exact analytical solution for the FGM in which thermophysical properties have certain profiles. Since the heat diffusion equation

$$\rho(z)\, c(z) \frac{\partial \theta(z, t)}{\partial t} = \frac{\partial}{\partial z}\left[\lambda(z) \frac{\partial \theta(z, t)}{\partial z}\right] \tag{16}$$

with the initial condition

$$\theta(z, 0) = 0 \tag{17}$$

and the boundary conditions

$$-\lambda_{\mathrm{F}} \frac{\partial \theta(-L, t)}{\partial z} = W(t), \qquad -\lambda_{\mathrm{R}} \frac{\partial \theta(0, t)}{\partial z} = 0 \tag{18}$$

can be described, after the Laplace transformation, as

$$\frac{d^2\Theta}{d\zeta^2} + \left(\frac{d \ln \Lambda}{d\zeta}\right)\left(\frac{d\Theta}{d\zeta}\right) - \eta_L^2 s\Theta = 0 \tag{19}$$

$$\left(\frac{\Lambda_{\mathrm{F}}}{\eta_L}\right)\left(\frac{\partial \Theta}{\partial \zeta}\right)_{\zeta=1} = W(s), \qquad \left(\frac{\Lambda_{\mathrm{R}}}{\eta_L}\right)\left(\frac{\partial \Theta}{\partial \zeta}\right)_{\zeta=0} = 0 \tag{20}$$

we can obtain an exact analytical solution when

$$\ln \Lambda = 2\alpha\zeta + \beta \tag{21}$$

where α and β are constants. In the above, use has been made of the variable ζ defined in Eq. (14), and the subscripts F and R, respectively, designate the front and rear surfaces; $\lambda_{\mathrm{F}} = \lambda(-L)$ and $\lambda_{\mathrm{R}} = \lambda(0)$.

For pulsewise heating, together with the positive root of $k\pi$ for the characteristic equation, the temperature response after the inverse Laplace transformation is expressed as

$$\theta(z, t) = \frac{Q\alpha e^{\alpha}}{\eta_L \Lambda_{\mathrm{F}} \sinh \alpha} V_{\mathrm{P}} \tag{22}$$

$$V_{\mathrm{P}} = 1 + 2 \sum_{k=1}^{\infty} (-1)^k \cos(k\pi\zeta)\, e^{-(k\pi)^2 \mathrm{Fo}} f_{\mathrm{P},k} \tag{23}$$

$$f_{\mathrm{P},k}=\frac{\sinh\alpha}{\alpha}e^{-\alpha\zeta-\alpha^2\mathrm{Fo}}\frac{(k\pi)^2}{(k\pi)^2+\alpha^2}\left[1+\frac{\alpha}{k\pi}\tan(k\pi\zeta)\right] \tag{24}$$

Note that for Λ in Eq. (21), Eq. (12) has a correction term,

$$\Phi_{\mathrm{P},k}=-\alpha\zeta+\frac{\alpha}{k\pi}\tan(k\pi\zeta) \tag{25}$$

which can be an approximate expression of a part of the correction factor $f_{\mathrm{P},k}$ at $\alpha\ll 1$.

For stepwise heating, we have

$$\theta(z,t)=\frac{\eta_L Q\alpha e^{\alpha}}{\Lambda_{\mathrm{F}}\sinh\alpha}V_{\mathrm{S}} \tag{26}$$

$$V_{\mathrm{S}}=\mathrm{Fo}+\frac{1+e^{-2\alpha\zeta}+2\alpha(\zeta-\coth\alpha)}{4\alpha^2}-2\sum_{k=1}^{\infty}\frac{(-1)^k\cos(k\pi\zeta)}{(k\pi)^2}e^{-(k\pi)^2\mathrm{Fo}}f_{\mathrm{S},k} \tag{27}$$

$$f_{\mathrm{S},k}=\frac{\sinh\alpha}{\alpha}e^{-\alpha\zeta-\alpha^2\mathrm{Fo}}\left\{\frac{(k\pi)^2}{(k\pi)^2+\alpha^2}\right\}^2\left[1+\frac{\alpha}{k\pi}\tan(k\pi\zeta)\right] \tag{28}$$

When $\alpha\ll 1$, the second term in Eq. (27) becomes $[-(1/6)+(\zeta^2/2)]$. Note that for Λ in Eq. (21), Eq. (13) has a correction term,

$$\Phi_{\mathrm{S},0}=0,\qquad \Phi_{\mathrm{S},k}=-\alpha\zeta+\frac{\alpha}{k\pi}\tan(k\pi\zeta) \tag{29}$$

which can be an approximate expression of a part of the correction factor $f_{\mathrm{S},k}$ at $\alpha\ll 1$.

5. NUMERICAL RESULTS

5.1. Comparisons Between Approximate and Analytical Solutions

Numerial calculations have been performed in order to compare the approximate solution with the exact analytical solution. In the following, we restrict ourselves to the pulse heating method because nearly the same results are anticipated for the step heating method.

Before numerical calculations, profiles of the heat-penetration coefficient Λ expressed by Eq. (21) are obtained. Figure 2 shows profiles of $(\Lambda/\Lambda_{\mathrm{R}})=\exp(2\alpha\zeta)$ as a function of ζ, with α taken as a parameter. Even at $\alpha=1$, the ratio of Λ_{F} and Λ_{R} becomes 7.39, the value of which is the same

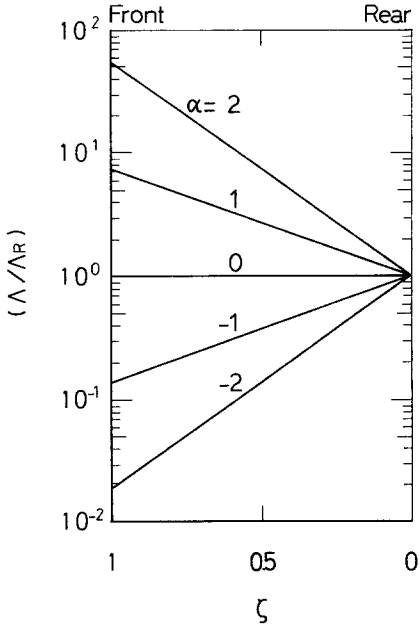

Fig. 2. Profile of the heat-penetration coefficient Λ in the FGM as a function of the normalized thermal diffusion time ζ, with α taken as a parameter.

order of magnitude as that for any combinations of conventional solid materials. In other words, as far as we consider the FGM which is constructed by conventional solid materials, it is sufficient to consider the situation where $-1 \leqslant \alpha \leqslant 1$.

As a first step, let us study the Fourier number $\mathrm{Fo}_{1/2}$ at which the temperature rise at the rear surface reaches 50% of its maximum rise. Figure 3 shows $\mathrm{Fo}_{1/2}$ as a function of α. The solid curve is obtained with the exact analytical solution of Eq. (23); the dashed line is the approximate solution of Eq. (12). When $\alpha = 0$, that is, the sample material is a single-layered material with no distribution in Λ, $\mathrm{Fo}_{1/2}$ becomes 0.1388. With increasing (or decreasing) α, $\mathrm{Fo}_{1/2}$ for the analytical solution decreases, while it remains constant for the approximate solution. Although about 6% error arises in $\mathrm{Fo}_{1/2}$ at $\alpha = \pm 1$, from the engineering point of view, this error can be acceptable since far greater errors may be encountered in the experiments.

Since the validity of the approximate solution of Eq. (12) at the rear surface is demonstrated, let us next investigate the temperature response inside the FGM. Following the above consideration, we choose $\alpha = \pm 1$. Figure 4 shows the temperature response as a function of Fo number, with

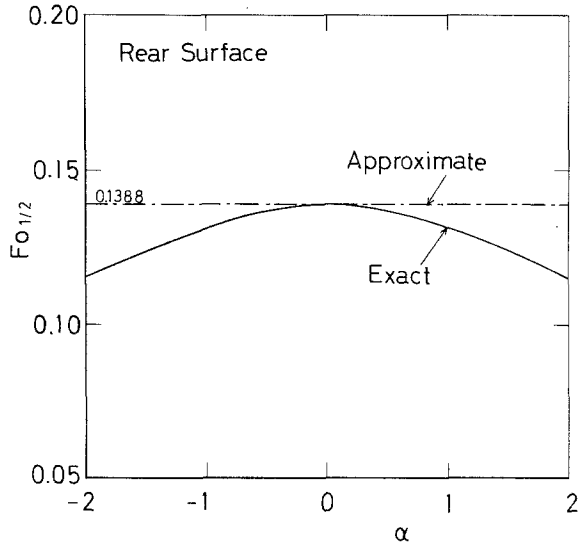

Fig. 3. The Fourier number $Fo_{1/2}$ at which the temperature rise at the rear surface reaches 50% of the maximum temperature rise at the rear, as a function of α. The solid curve was obtained with the exact analytical solution; the dashed line was obtained with the approximate solution.

ζ taken as a parameter; solid curves are the analytical solutions, dashed curves the approximate solutions without correction terms $\Phi_{P,k}$, and long/short-dashed curves the approximate solutions with $\Phi_{P,k}$. When $\zeta = 0$ and 0.25, the approximate solutions represent the analytical solutions reasonably well. Furthermore, the approximate solution without $\Phi_{P,k}$ is closer to the analytical solution than that with $\Phi_{P,k}$. However, when $\zeta = 0.5$ or greater, we see that we cannot use the approximate solutions anymore to evaluate the temperature response in the FGM. This is attributed to the fact that the assumption $A_{m/m+1} \approx 1$ cannot be adopted because the change of A near the front surface is steeper than that near the rear surface.

In order to clarify further the deviations of the approximate solutions from the analytical solution, the Fourier number $Fo_{1/2}$ at which the inside temperature rise reaches 50% of its maximum rise at the rear surface is obtained. Figure 5 shows the deviation of the Fo numbers as a function of ζ, with α taken as a parameter; dashed curves are the approximate solutions without $\Phi_{P,k}$ and dot-dash curves are those with $\Phi_{P,k}$. With increasing ζ, the deviation of the approximate solution without $\Phi_{P,k}$ decreases from a certain positive value at $\zeta = 0$ to a negative value, while that of the approximate solution with $\Phi_{P,k}$ increases. As a result, the applicable range

of the approximate solution without $\Phi_{P,k}$ is wider than that of the approximate solution with $\Phi_{P,k}$. For $\alpha = \pm 1$, the approximate solution without $\Phi_{P,k}$ can be used for the evaluation of the temperature response, up to about $\zeta = 0.34$ in the FGM, within 6% error.

It may be imformative to discuss here the relation between the normalized diffusion time ζ and the normalized length $z/(-L)$ in the FGM when the profile function of the thermal diffusivity a is given as

$$a = a_R + (a_F - a_R)[z/(-L)]^p \tag{30}$$

For integer exponents up to 2, there exist analytical expressions for ζ:

$$\text{at } p = 0, \quad \zeta = \left(\frac{z}{-L}\right) \tag{31}$$

$$\text{at } p = 1, \quad \zeta = \frac{\sqrt{1+y}-1}{\sqrt{1+y_L}-1}; \qquad y = y_L\left(\frac{z}{-L}\right); \quad y_L = \frac{a_F - a_R}{a_R} \tag{32}$$

$$\text{at } p = 2, \quad \zeta = \frac{\ln(\sqrt{1+y^2}-y)}{\ln(\sqrt{1+y_L^2}-y_L)}; \quad y = y_L\left(\frac{z}{-L}\right); \quad y_L^2 = \frac{a_F - a_R}{a_R} \tag{33}$$

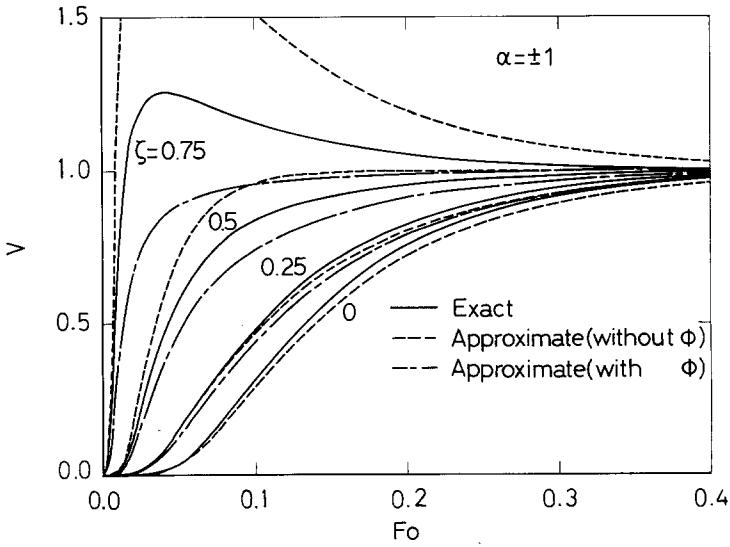

Fig. 4. Normalized temperature response as a function of the Fourier number, with the position inside the FGM taken as a parameter; $\alpha = \pm 1$. Solid curves were obtained with the exact analytical solution, dashed curves were obtained with the approximate solution without correction terms, and long/short-dash curves were obtained with the approximate solution with correction terms.

As $y_L \to \infty$, $\zeta = \sqrt{z/(-L)}$ for $p=1$ and $\zeta = 1$ for $p=2$. When $y_L = 0$, $\zeta = z/(-L)$ regardless of the values of p. These results are shown in Fig. 6.

5.2. Comparisons Between the Approximate Solution for FGM and the Solution for Multilayered Material

Here we evaluate the validity of the approximate solution without $\Phi_{P,k}$ in Eq. (12), comparing it with the solution for the multilayered material in Eq. (2). As a sample material, we consider an FGM which consists of Fe and TiO_2 whose thermophysical properties are listed in Table I. We assume that the front surface is made of Fe, that the rear surface is TiO_2, and that the mixture ratio of these components in the FGM is a linear function of the thickness, as shown in Fig. 7. In this calculation, use has been made of the following relation for the thermophysical properties

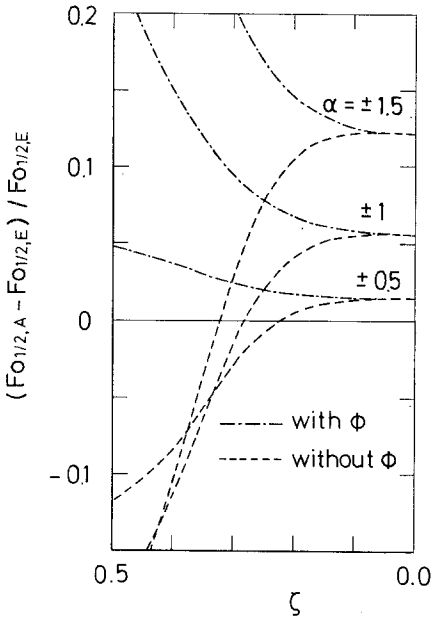

Fig. 5. Deviation of the Fourier numbers $(Fo_{1/2,A} - Fo_{1/2,E})/Fo_{1/2,E}$ as a function of the position inside the FGM, with α taken as a parameter. Subscripts A and E respectively designate approximate and exact analytical solutions. Dashed curves were obtained with the approximate solution without correction terms; dot-dash curves were obtained with the approximate solution with correction terms.

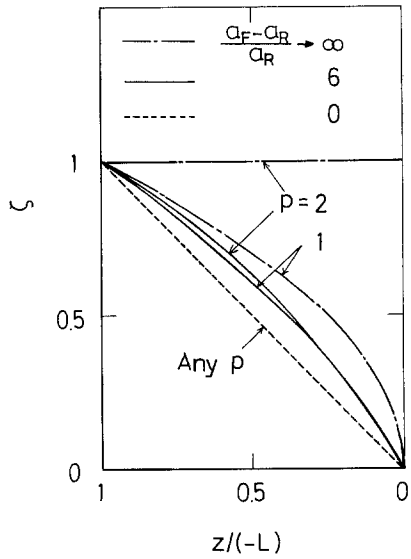

Fig. 6. The normalized thermal diffusion time ζ as a function of the normalized length from the rear surface, with the exponent to express the profile function of the thermal diffusivity, and the ratio of the thermal diffusivities at the front and rear surfaces taken as parameters.

of the material which consists of Component I (Fe) with the mixture ratio X and Component II (TiO_2) with the mixture ration $(1-X)$ as

$$\rho = \rho_I X + \rho_{II}(1-X), \qquad \rho c = \rho_I c_I X + \rho_{II} c_{II}(1-X) \tag{34}$$

$$\frac{1}{\lambda} = \frac{X}{\lambda_I} + \frac{1-X}{\lambda_{II}}, \qquad a = \frac{\lambda}{\rho c} \tag{35}$$

Table I. Thermophysical Properties of Components in an FGM Consisting of Fe and TiO_2

Component	Material	Heat-penetration coefficient ($kJ \cdot m^{-2} \cdot K^{-1} \cdot s^{-1/2}$)	Thermal diffusivity ($m^2 \cdot s^{-1}$)
I	Fe	15	2.1×10^{-5}
II	TiO_2	5	3.0×10^{-6}

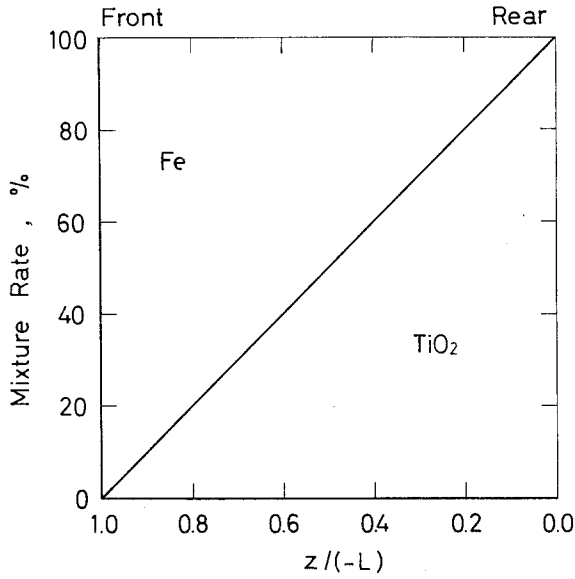

Fig. 7. Profile of the mixture ratio as a function of the normalized length $z/(-L)$ from the rear surface.

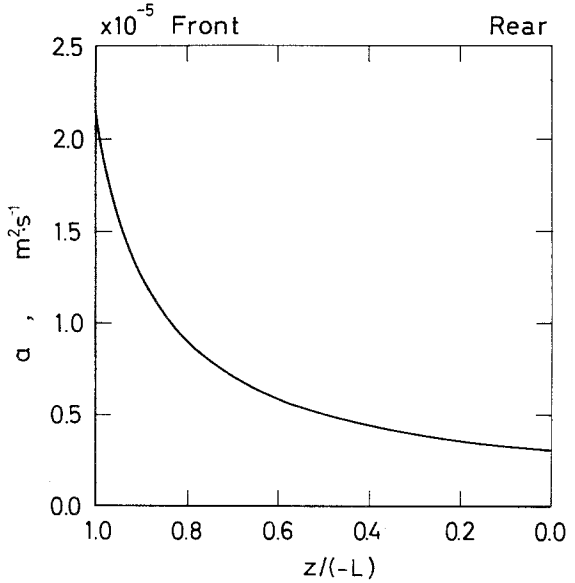

Fig. 8. Profile of the thermal diffusivity a as a function of the normalized length $z/(-L)$ from the rear surface.

Figure 8 shows the profile of the thermal diffusivity a for the FGM whose mixture ratio is shown in Fig. 7; Fig. 9 shows the profile of the heat-penetration coefficient A. When we use the solution for the multilayered material, discretization for the thermophysical properties is made; thickness of each layer is set to be the same.

Figure 10 shows the Fourier number $Fo_{1/2}$ obtained from the temperature response at the rear surface as a function of the number n of layers in the sample material. We see that with an increasing number of layers, $Fo_{1/2}$ gradually decreases. Because of the limitation of the memory capacity of a personal computer, results obtained with Eq. (2), which are shown by squares in Fig. 10, can be obtained only for the multilayered materials with up to 15 layers. Although numerical results are limited, we see a general trend that $Fo_{1/2}$ decreases and reaches a certain value. Furthermore, $Fo_{1/2}$ for $n=5$ is 3% larger than that for $n=15$; $Fo_{1/2}$ for $n=8$ is 1% larger than that for $n=15$. That is, we can say that we can investigate the temperature response of FGM considering that it is composed of an eight-layered material.

In Fig. 10, it is also shown a result based on Eq. (12); $Fo_{1/2}=0.1388$. Although Eq. (12) is approximate, it predicts the temperature response within 6% error when we compare it with that for $n=15$. If this error

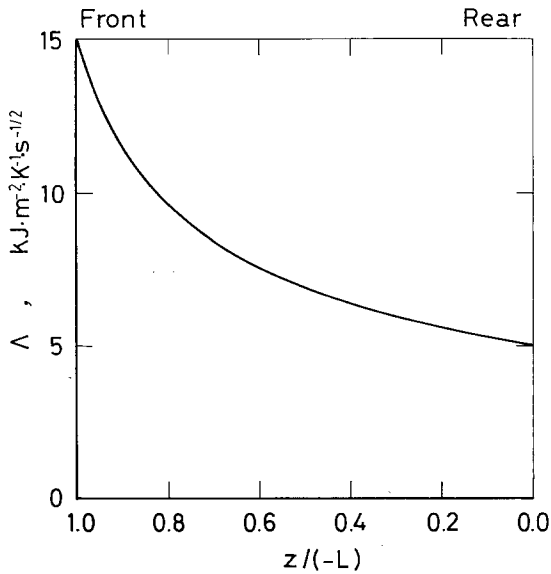

Fig. 9. Profile of the heat-penetration coefficient A as a function of the normalized length $z/(-L)$ from the rear surface.

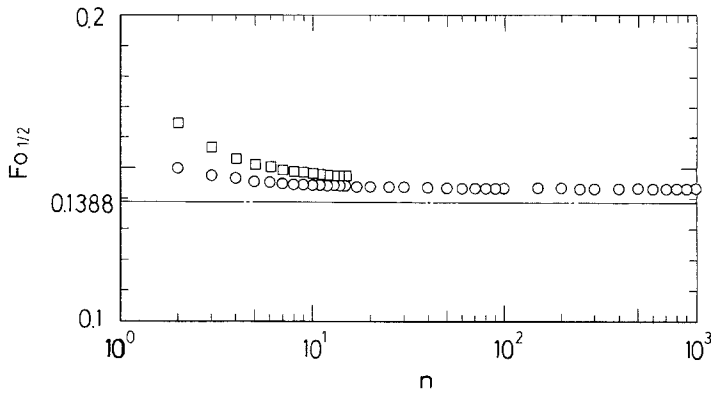

Fig. 10. The Fourier number $Fo_{1/2}$ at which the temperature rise at the rear surface reaches 50% of the maximum temperature rise. The squares represent the results obtained with the solution for the multilayered material, the circles represent the results obtained with the selection method, and the dash-dot line was obtained with the approximate solution.

is acceptable, the approximate solution can be used to evaluate the heat-shielding properties of FGM.

In order to demonstrate further the effect of the number of layers in the sample material, selection of parameters χ's has been made. This selection is made to pick up χ's in which negative sign does not exist or appears once for the calculation of $\alpha_{j,m}\alpha_{j,m+1}$ in Eq. (5). This selection reflects the same situation as that for the perturbation method in the Appendix. With this selection, number of χ's is reduced from 2^{n-1} to n. In Fig. 10, results with this selection method are also shown by circles. We see that $Fo_{1/2}$ decreases and reaches a certain value with an increasing number of the layers; $Fo_{1/2}$ for $n=8$ is 1% larger than that for $n=1000$. For an eight-layered material, $Fo_{1/2}$ with this selection method is 3% smaller than that with Eq. (2). The deviation is nearly the same order of magnitude for a 15-layered material. This selection method can further offer us a fairly accurate evaluation when the approximate solution is considered to be a somewhat crude evaluation.

6. CONCLUDING REMARKS

In the present study, the temperature response in a functionally gradient material (FGM) which is subjected to transient heating is investigated, in order to obtain basic information to confirm the measurement principles in the application of transient methods to FGM. The validity of the approximate solution for the temperature response in FGM

is evaluated. For this evaluation, the approximate solution obtained under the equi-heat-penetration assumption is compared with the exact analytical solution which can exist when the thermophysical properties have certain profiles in the FGM. It is shown that although the solution is approximate, it helps to evaluate the temperature response, especially near the rear surface of FGM, for an FGM constructed from conventional solid materials.

In order to evaluate further the validity of the approximate solution, it is compared with the solution for the multilayered material, with an FGM composed of Fe and TiO_2 as the sample material. Although the temperature response varies depending on the number of layers, it has been noted that an eight-layered material can be regarded as an FGM, as far as the temperature response is concerned. Furthermore, the approximate solution can predict the temperature response within 6%. From the engineering point of view, because of its simplicity and fair degree of agreement, the approximate solution is anticipated to be used not only for qualitative but also for quantitative prediction of the temperature response near the rear surface of the FGM.

APPENDIX: DERIVATION OF APPROXIMATE TEMPERATURE RESPONSE IN FGM WITH THE PERTURBATION METHOD

The perturbation method is applied to Eqs. (2) and (4), in order to obtain approximate expressions for the temperature response in FGM with higher-order approximation. If we put

$$\Lambda_{m/m+1} \approx 1 - \left(\frac{d \ln \Lambda}{dz}\right)_m \delta z \equiv 1 - 2\varepsilon_m \tag{A1}$$

we have

$$\chi_1 \approx \prod_{m=1}^{n-1} 2(1-\varepsilon_m) \approx 2^{n-1}\left(1 - \sum_{m=1}^{n-1} \varepsilon_m\right) \tag{A2}$$

and χ's in which negative sign appears once are expressed as

$$\begin{aligned} \chi_{\textcircled{j}} &\approx \left[\prod_{m=1}^{j-1} 2(1-\varepsilon_m)\right](-2\varepsilon_j)\left[\prod_{m=j+1}^{n-1} 2(1-\varepsilon_m)\right] \\ &\approx -\varepsilon_j \chi_1 \end{aligned} \tag{A3}$$

As for ω's, they are

$$\omega_1 = \sum_{m=1}^{n} \eta_{m/n} \qquad \omega_{\textcircled{j}} = \omega_1 - 2 \sum_{m=j+1}^{n} \eta_{m/n} \tag{A4}$$

In the same way, χ^*'s and ω^*'s are expressed as follows:

$$\chi_1^* \approx 2^{n-i}\left(1-\sum_{m=i}^{n-1}\varepsilon_m\right), \qquad \chi_{\textcircled{i}}^* \approx -\varepsilon_j \chi_1^* \tag{A5}$$

$$\omega_1^* = \eta_{i/n}^* + \sum_{m=i+1}^{n}\eta_{m/n} \qquad \omega_{\textcircled{i}}^* = \omega_1^* - 2\sum_{m=j+1}^{n}\eta_{m/n} \tag{A6}$$

If we regard that the kth positive root for the lowest-order approximation is $\gamma_k\omega_1 = k\pi$ and compare terms of the same order of ε, the characteristic solution is obtained as

$$\gamma_k \approx \frac{1}{\omega_1}\left[k\pi - \sum_{j=1}^{n-1}\varepsilon_j \sin\left(\frac{2k\pi}{\omega_1}\sum_{m=j+1}^{n}\eta_{m/n}\right)\right] \tag{A7}$$

Since we can express as

$$\sum_{j=1}^{2^n-1}\omega_j\chi_j \approx \omega_1\chi_1\left[1-\sum_{j=1}^{n-1}\varepsilon_j\left(1-\frac{2}{\omega_1}\sum_{m=j+1}^{n}\eta_{m/n}\right)\right] \tag{A8}$$

$$\sum_{j=1}^{2^n-1}\omega_j\chi_j\cos(\gamma_k\omega_j) \approx (-1)^k\omega_1\chi_1\left[1-\sum_{j=1}^{n-1}\varepsilon_j\left(1-\frac{2}{\omega_1}\sum_{m=j+1}^{n}\eta_{m/n}\right)\times\cos\left(\frac{2k\pi}{\omega_1}\sum_{m=j+1}^{n}\eta_{m/n}\right)\right] \tag{A9}$$

$$e^{-(\gamma_k\omega_1)^2\mathrm{Fo}} \approx e^{-(k\pi)^2\mathrm{Fo}}\left[1+(2k\pi\mathrm{Fo})\sum_{j=1}^{n-1}\varepsilon_j \times\sin\left(\frac{2k\pi}{\omega_1}\sum_{m=j+1}^{n}\eta_{m/n}\right)\right] \tag{A10}$$

$$\sum_{j=i}^{i-1+2^{n-i}}\chi_j^*\cos(\gamma_k\omega_j^*) \approx \chi_1^*\cos\left(\frac{k\pi}{\omega_1}\omega_1^*\right)\left[1-\sum_{j=i}^{n-1}\varepsilon_j\cos\left(\frac{2k\pi}{\omega_1}\sum_{m=j+1}^{n}\eta_{m/n}\right)+\left(\frac{\omega_1^*}{\omega_1}\right)\tan\left(\frac{k\pi}{\omega_1}\omega_1^*\right)\sum_{j=1}^{n-1}\varepsilon_j\sin\left(\frac{2k\pi}{\omega_1}\sum_{m=j+1}^{n}\eta_{m/n}\right)-\tan\left(\frac{k\pi}{\omega_1}\omega_1^*\right)\sum_{j=i}^{n-1}\varepsilon_j\sin\left(\frac{2k\pi}{\omega_1}\sum_{m=j+1}^{n}\eta_{m/n}\right)\right] \tag{A11}$$

$$\sum_{j=i}^{i-1+2^{n-i}}\chi_j^* \approx \chi_1^*\left(1-\sum_{j=i}^{n-1}\varepsilon_j\right) \tag{A12}$$

the temperature response in Eq. (2) for pulsewise heating and that in Eq. (4) for stepwise heating can be expressed approximately with perturbed terms. Furthermore, if we consider the situation of infinitesimal discretiza-

tion, the above summations can be expressed in the form of integrations; that is,

$$\lim_{n\to\infty}\left(\frac{1}{\omega_1}\sum_{m=j+1}^{n-1}\eta_{m/n}\right)=\left(\int_z^0\frac{dz}{\sqrt{a}}\right)\Big/\left(\int_{-L}^0\frac{dz}{\sqrt{a}}\right)\equiv\zeta \tag{A13}$$

$$\lim_{n\to\infty}\left(\frac{\omega_1^*}{\omega_1}\right)=\left(\int_z^0\frac{dz}{\sqrt{a}}\right)\Big/\left(\int_{-L}^0\frac{dz}{\sqrt{a}}\right)\equiv\zeta \tag{A14}$$

Then Eq. (2) for pulsewise heating becomes

$$V_{\mathrm{P}}=1+2\sum_{k=1}^{\infty}(-1)^k\cos(k\pi\zeta)\,e^{-(k\pi)^2\mathrm{Fo}}(1+\Phi_{\mathrm{P},k}) \tag{A15}$$

$$\begin{aligned}\Phi_{\mathrm{P},k}=&-\frac{1}{2}\int_{-L}^0\left(\frac{d\ln\Lambda}{dz}\right)[(1-2\zeta)\{1-\cos(2k\pi\zeta)\}-(2k\pi\mathrm{Fo})\sin(2k\pi\zeta)]\,dz\\&+\frac{\zeta\tan(k\pi\zeta)}{2}\int_{-L}^0\left(\frac{d\ln\Lambda}{dz}\right)\sin(2k\pi\zeta)\,dz\\&+\frac{1}{2}\int_z^0\left(\frac{d\ln\Lambda}{dz}\right)[1-\cos(2k\pi\zeta)]\,dz\\&-\frac{\tan(k\pi\zeta)}{2}\int_z^0\left(\frac{d\ln\Lambda}{dz}\right)\sin(2k\pi\zeta)\,dz\end{aligned} \tag{A16}$$

We can also express Eq. (A16) in another form, as

$$\begin{aligned}\Phi_{\mathrm{P},k}=&\frac{1}{\eta_L}\int_{-L}^0\left(\frac{\ln\Lambda}{\sqrt{a}}\right)[1+\{2(k\pi)^2\ \mathrm{Fo}-1\}\cos(2k\pi\zeta)\\&\qquad-k\pi(1-2\zeta)\sin(2k\pi\zeta)]\,dz\\&+\frac{(k\pi\zeta)\tan(k\pi\zeta)}{\eta_L}\int_{-L}^0\left(\frac{\ln\Lambda}{\sqrt{a}}\right)\cos(2k\pi\zeta)\,dz\\&+\frac{k\pi}{\eta_L}\int_z^0\left(\frac{\ln\Lambda}{\sqrt{a}}\right)\sin(2k\pi\zeta)\,dz\\&-\frac{(k\pi)\tan(k\pi\zeta)}{\eta_L}\int_z^0\left(\frac{\ln\Lambda}{\sqrt{a}}\right)\cos(2k\pi\zeta)\,dz\end{aligned} \tag{A17}$$

When the profile function of the heat-penetration coefficient Λ has a form expressed by Eq. (20), Eq. (A16) becomes

$$\Phi_{\mathrm{P},k}=-\alpha\zeta+\frac{\alpha}{k\pi}\tan(k\pi\zeta) \tag{A18}$$

which is an approximate form of $(f_{\mathrm{P},k}-1)$ when $\alpha\ll1$; cf. Eq. (23).

For stepwise heating, Eq. (4) becomes

$$V_S = \mathrm{Fo} - \frac{1+\Phi_{S,0}}{6} + \frac{\zeta^2}{2} - 2\sum_{k=1}^{\infty} \frac{(-1)^k \cos(k\pi\zeta)}{(k\pi)^2} e^{-(k\pi)^2 \mathrm{Fo}} (1+\Phi_{S,k}) \tag{A19}$$

$$\Phi_{S,0} = 2\int_{-L}^{0} \left(\frac{d\ln\Lambda}{dz}\right) \zeta(1-\zeta)(1-2\zeta)\, dz \tag{A20}$$

$$\Phi_{S,k} = -\frac{1}{2}\int_{-L}^{0} \left(\frac{d\ln\Lambda}{dz}\right) \left[(1-2\zeta)\{1-\cos(2k\pi\zeta)\} - \frac{2\{(k\pi)^2\,\mathrm{Fo}+1\}}{k\pi} \sin(2k\pi\zeta) \right] dz + \frac{\zeta\tan(k\pi\zeta)}{2} \int_{-L}^{0} \left(\frac{d\ln\Lambda}{dz}\right) \sin(2k\pi\zeta)\, dz + \frac{1}{2}\int_{z}^{0} \left(\frac{d\ln\Lambda}{dz}\right) [1-\cos(2k\pi\zeta)]\, dz - \frac{\tan(k\pi\zeta)}{2} \int_{z}^{0} \left(\frac{d\ln\Lambda}{dz}\right) \sin(2k\pi\zeta)\, dz \tag{A21}$$

We can also express Eqs. (A20) and (A21) in another form, as

$$\Phi_{S,0} = -\frac{2}{\eta_L}\int_{-L}^{0} \left(\frac{\ln\Lambda}{\sqrt{a}}\right) (1-6\zeta+6\zeta^2)\, dz \tag{A23}$$

$$\Phi_{S,k} = \frac{1}{\eta_L}\int_{-L}^{0} \left(\frac{\ln\Lambda}{\sqrt{a}}\right) [1+\{2(k\pi)^2\,\mathrm{Fo}+1\}\cos(2k\pi\zeta) - k\pi(1-2\zeta)\sin(2k\pi\zeta)]\, dz + \frac{(k\pi\zeta)\tan(k\pi\zeta)}{\eta_L} \int_{-L}^{0} \left(\frac{\ln\Lambda}{\sqrt{a}}\right) \cos(2k\pi\zeta)\, dz + \frac{k\pi}{\eta_L}\int_{z}^{0} \left(\frac{\ln\Lambda}{\sqrt{a}}\right) \sin(2k\pi\zeta)\, dz - \frac{(k\pi)\tan(k\pi\zeta)}{\eta_L} \int_{z}^{0} \left(\frac{\ln\Lambda}{\sqrt{a}}\right) \cos(2k\pi\zeta)\, dz \tag{A23}$$

When the heat-penetration coefficient Λ is expressed as Eq. (20), Eqs. (A20) and (A21) are

$$\Phi_{S,0}=0, \qquad \Phi_{S,k}=-\alpha\zeta+\frac{\alpha}{k\pi}\tan(k\pi\zeta) \tag{A24}$$

Here $\Phi_{S,k}$ is an approximate form of $(f_{S,k}-1)$ when $\alpha \ll 1$; cf. Eq. (27).

ACKNOWLEDGMENT

This work was supported in part by the Foundation for Promoting Science and Technology on Functionally Gradient Materials, a contract funded through the National Aerospace Laboratory and sponsored by the Science and Technology Agency, Japan.

NOMENCLATURE

a	Thermal diffusivity
c	Specific heat
Fo	Fourier number $[=at/l^2]$
f	Correction factor
L	Thickness of the sample material
l	Thickness of the layer
n	Number of layers in the sample material
p	Exponent in the profile function of a
Q	Heat input per unit area
s	Parameter in the Laplace transformation
t	Time
V	Normalized temperature response
W	Heat input function
X	Mixture ratio
y	Variable
z	Distance

Greek Symbols

α	Constant in the profile function of Λ
$\alpha_{j,m}$	± 1
β	Constant in the profile function of Λ
γ	Positive root of the characteristic equation
ε	Perturbed term
ζ	Normalized thermal diffusion time defined in Eq. (14)

η Thermal diffusion time $[= l/\sqrt{a}]$
η_L Total thermal diffusion time defined in Eq. (14)
Θ Laplace transform of the temperature rise
θ Temperature rise
Λ Heat-penetration coefficient $[= \lambda/\sqrt{a}]$
λ Thermal conductivity
ρ Density
Φ Correction term
χ Parameter defined in Eqs. (5) and (6)
ω Parameter defined in Eqs. (5) and (6)

Subscripts

F Front surface
i Value of ith layer
i/j (Quantity of the ith layer) divided by (quantity of the jth layer)
P Pulsewise heating method
R Rear surface
S Stepwise heating method
I Component I
II Component II

Superscript

* Inside the layer

REFERENCES

1. N. Araki, A. Makino, and J. Mihara, *Int. J. Thermophys.* **13**:331 (1992).
2. N. Araki, A. Makino, T. Ishiguro, and J. Mihara, *Int. J. Thermophys.* **13**:515 (1992).